Colony and Pattern Formation in *Diatoma tenuis*

Thomas Harbich

Independent Researcher, Am Brüdenrain 18, 71554 Weissach im Tal, Germany

Author links:

https://orcid.org/0000-0002-9151-4052
https://www.researchgate.net/profile/Thomas_Harbich
https://www.diatoms.de/en/

Abstract
The araphid diatom *Diatoma tenuis* C.Agardh forms chain-like colonies that can have different structures. Populations consisting of one or more connected star-shaped formations, each containing three diatoms, and transitional forms between these structures are considered. It is shown that formation and reproduction of star-like structures can be described by a deterministic Lindenmayer system. The formation of larger aggregates is prevented by a breakage mechanism restricted to specific connecting points in the colony. An extension of the Lindenmayer system to include information on the age of potential break sites allows the simulation of chain sizes with hypothetical probabilities for the breaks. This reveals that the breakage mechanism has a characteristic temporal behavior in which the probability of breakage is low over one generation time and then increases strongly. The occurrence of transitional forms which is not described by the Lindenmayer system is a consequence of imperfect synchronism of cell divisions. It is discussed based on observational data. Essential for a low sinking speed of the colonies is the symmetry of the star-shaped structures. The distribution of angles between neighboring diatoms is studied and the increase in sinking speed due to deviations from perfect symmetry is estimated. Observations show that after cell divisions favorable angles are reached in a time that is short compared to the generation time. The formation of the colony structures and the mechanisms required for this are discussed in the context of evolutionary advantage.

Keywords: *Diatoma tenuis*, colony formation, pattern formation, stellate diatom colonies, Lindenmayer system

1.1 Introduction

Diatoms form a class of unicellular algae found in almost all aquatic habitats as well as in soil. They possess an exoskeleton (frustule) of hydrated silicate, consisting of two halves of different sizes called thecae. The larger is called epitheca, the smaller

hypotheca. Both comprise a valve and the cingulum, a number of associated girdle bands. When diatoms reproduce by vegetative division, the thecae of the parent cell are retained and the smaller hypothecae are newly formed to each. These relationships were discovered by MacDonald 1869 [1.25] and Pfitzer 1869 [1.33] and have been demonstrated for many species (e.g. Locker [1.24]). Details, particularly on morphology, can be found in Round [1.39], for example. If, after such a division, the cells remain mechanically connected for a period longer than the generation time, a clonal colony is formed. Rimet [1.38] gives an overview of the forms that such colonies take. In the formation of colonies of pennate diatoms, the case occurs in some species that after cell division the diatoms fold apart from the parallel formation but remain connected at their opposed poles by a pad of extracellular polymeric substances (EPS) [1.3]. The colonies are then typically stellate or zig-zag-shaped. Star-shaped colonies are formed, for example, by the species of the genus *Asterionella*. Stellate and zig-zag-colonies occur in the genera *Tabellaria* and *Diatoma*. *Diatoma tenuis* C.Agardh ([1.1] [1.35]) forms zig-zag-shaped colonies in which star-shaped structures may also be inserted [1.19]. Some populations exclusively form colonies consisting of star-shaped structures with three diatoms or of several such connected stars (see images in [1.4]). We will restrict ourselves to these colony forms, which can be associated with a planktonic way of life. Apart from that, *D. tenuis* also occurs epiphytically and (more rarely) benthically [1.19]. An example of a single and a double star structure is shown in Figure 1.1. In addition, transitional forms between these structures are often found.

The life-forms can only be understood in the context of the life history strategy. Zig-zag-shaped colonies, such as *Diatoma vulgaris*, attached to one or more diatoms by

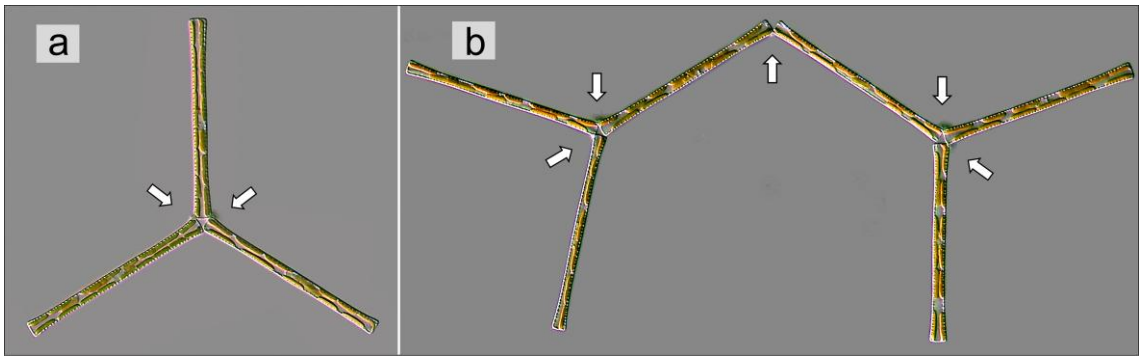

Figure 1.1 DIC images of *D. tenuis* colonies. The arrows point to the connecting EPS pads. (a) structure consisting of three diatoms. (b) structure consisting of six diatoms, which can be thought as two connected star-shaped colonies.

means of adhesive pads [1.6] to the substrate, allow diatoms, especially in flowing waters, to protrude far into the water body, improving access to light and nutrients. This requires an adequate length and stability of the chains. Phytoplankton must have

sufficient floatability, i.e. low sinking speed, to be able to photosynthesize for a sufficiently long time [1.28] and to reproduce. For this purpose, it is important to achieve good buoyancy. On the other hand, faster sinking of diatoms that have reached a resting state after a diatom bloom may also be advantageous [1.40]. To this end, increased mucus secretion can cause rapidly sinking aggregates to form, and some species are able to regulate their buoyancy to control sinking rate and position in the water column ([1.2] [1.40] [1.12]). For the possibility of a long stay in the surface area, the shape of the diatoms plays a central role. Several marine species have appendages such as chitin fibres or spines that reduce sinking speed (for a review [1.28]). In the genera *Chaetoceros* and *Bacteriastrum*, robust extensions, so-called setae, are found which serve to mechanically connect the diatoms and assist floatation ([1.42] [1.41]). Conway and Trainor [1.7] have shown on green algae of the genus *Scenedesmus* that strains with spines sank more slowly than those with the spines removed. Walsby and Xypolyta [1.44] experimentally demonstrated that the sinking rate of *Thalassiosira fluviatilis* increases by a factor of 1.7 when the chitin fibrils are removed.

An alternative to reduce the sinking speed is the formation of star-shaped colonies in which diatoms are directed radially outward from a center. Experimental studies with models of *Asterionella*, show that such colonies have a sinking rate that decreases with the number of diatoms involved in the stellate formation [1.32]. Moreover, the experiments prove that regular structures with identical opening angles are advantageous [1.32]. It can be reasonably postulated that this is also the background for the separate and connected star-shaped structures in *D. tenuis*. A low sinking speed is only given for smaller colonies, which leads to the question of a mechanism to limit the chain length. Gherardi et al. have studied the chain lengths of the colony-forming species *Chaetoceros decipiens* and *Phaeodactylum tricornutum* experimentally and theoretically [1.14]. They use a stochastic model, and in the case of *Chaetoceros decipiens* they consider a cell-to-cell communication process likely.

In this work, the morphogenesis in the observed star-shaped structures of *D. tenuis* will be studied. The focus is on the rules that lead to the development and reproduction of such structures. Essential to the appearance is the location of the connection points, which can be investigated by the same methods we used in [1.16] for explaining the formation processes in *D. vulgaris*. To understand the colony size constraints, the possible fracture locations and the rupture behavior at these sites need to be modelled. For the question to what extent transitional forms between star-shaped

colonies occur, the synchronicity of cell divisions has to be investigated, because connected stellate structures in large numbers can only form if the durations of cell divisions do not deviate too much from the mean. Against the background of the evolutionary advantage of the structures, the degree of symmetry achieved and its effect on the sinking speed is of further importance. In this context, the timing behavior of the opening of the angles between neighboring diatoms needs to be addressed as well. Out of consideration are deeper chemical or mechanical mechanisms.

1.2 Materials and Methods

1.2.1 Cultivation

Some diatom colonies of the species *D. tenuis* were sampled from the water body of the river Neckar (Germany 49°04'41.8 N 9°09'17.9 E) on 18. October 2021. The typical apical length was 73 µm. The colonies were made up entirely of single and compound stellate structures. The appearance of this planktonic diatom in the flowing water can probably be explained by upstream barrages. *D. tenuis* was cultured in polystyrene Petri dishes and grown in an f/2 medium according to Guillard [1.15] at light intensities between 200 lx and 500 lx. A fluorescent lamp with a radiation temperature of 6000 K served as illumination, with the light phase lasting 11 hours and the dark phase 13 hours. The ambient temperature was 19° C to 21° C. Under these conditions, it is sufficient to inoculate a new batch culture with diatoms every three weeks. However, since most observations required a low density of diatoms, it proved convenient to inoculate new cultures weekly.

1.2.2 Recording technique

The study of dynamic processes requires observation times of several hours to several days. They were recorded in the cultures using an inverted microscope (Zeiss Axiovert A1). Statistical data (colony shapes, angles between neighboring diatoms) were collected in sedimented cultures based on image series, because a sufficient number of objects is present there and disturbing influences from external forces can be eliminated to a large extent. Images that required high resolution (e.g. to identify the species or to visualize the EPS pads) were taken using an upright microscope (Zeiss Axioplan).

1.2.3 Notation of concatenation, types of concatenation and processes of splitting

The basis for the analysis of the structure of zig-zag colonies, as well as stellate colonies is a notation, which allows to describe the sequence of connections. Figure 1.2a shows a hypothetical short diatom chain or fragment of a chain in girdle band view, with the EPS pads indicated by small circle segments. For the definition of the notation, it should not matter whether this sequence of connections exists in a species in nature. Since only connectivity is considered, the angles between diatoms are irrelevant here. For star-shaped colonies, the angles are reduced for the purpose of illustration.

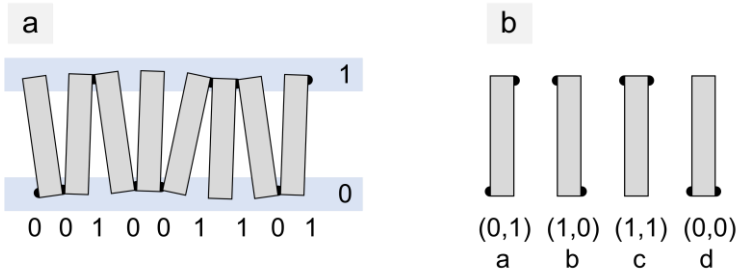

Figure 1.2 (a) Exemplary colony consisting of eight diatoms with the binary notation of the location of the EPS-pads in a selected position. (b) The four possible types *a*, *b*, *c* and *d* with assignment to the binary notation.

The position of the chain to the viewer is horizontal, otherwise arbitrary, but fixed. One can distinguish between an upper lower band and assign the position of the EPS pads to them. By indexing the connection with 1 if the pads are at the upper band and with 0 otherwise, a binary sequence is obtained, which characterizes the sequence for a given view unambiguously and without redundancies. Except at the ends, an EPS pad corresponds to a connection point. Light microscopically, the EPS pads are usually not recognizable at the ends, so that initially no indices can be assigned to them.

In modeling, it proves convenient to consider successive pairs of identifiers, each enclosing a diatom, and give them a new identifier. In this manner, the 2-tuple (0,1) characterizes a diatom of type a, as shown on the left in Figure 1.2b. Each diatom is assigned a type *a*, *b*, *c*, or *d* in this way. Note also here that the identifiers change when you rotate or mirror the chain. As successive 2-tuples always have a binary index in common, the possible sequences of two elements are *ab*, *ac*, *ba*, *bd*, *cc*, *cb*, *dd*, and *da*. Thus, an alternative description of the chain in Figure 1.2a is the string *dabdacba*. Types *a* and *b* have the pads at diagonally opposite points of the diatom and shall be referred to as "diagonal types". Correspondingly, *c* and *d* are called non-diagonal types.

This nomenclature was introduced in [1.16] to model the formation of *D. vulgaris* colonies. It is essential that the notation presented does not restrict the possible processes of division, nor does it suggest any such process.

When a diatom divides, a new contact point is formed between the daughter cells, which is assigned either the index 0 or 1. In Figure 1.3, the possible processes are shown in the nomenclature according to Figure 1.2b and numbered by Roman numerals.

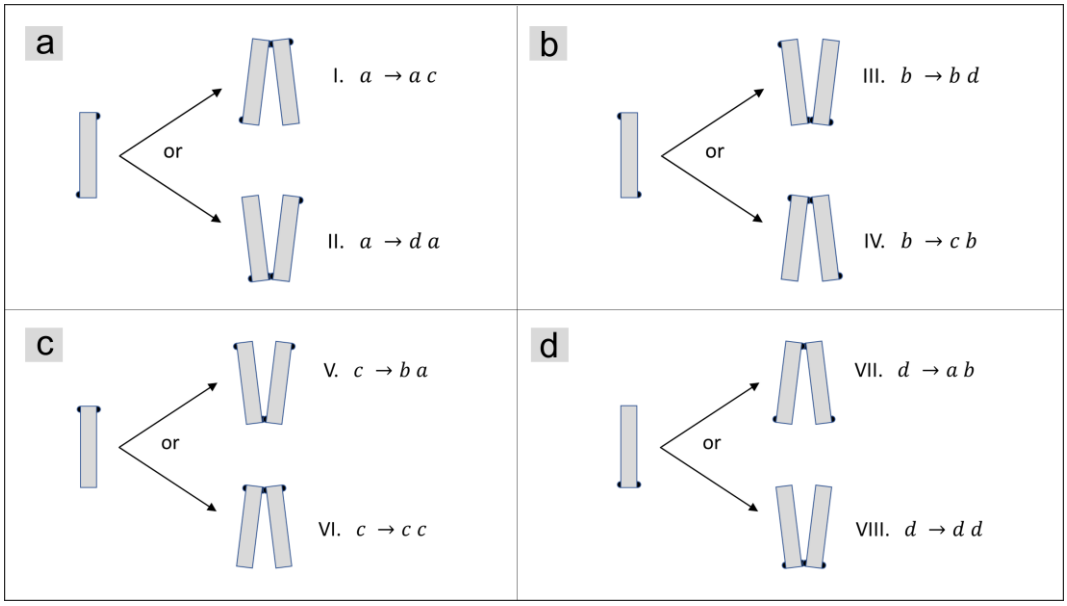

Figure 1.3 (a) to (d) show the possibilities of a division of the four elementary types.

Since a particular view of the horizontally oriented colony was chosen, it is of importance how the processes transform under a different choice. If one rotates a chain by 180° with a vertical view on it, the types a and b remain invariant, while c and d interchange. The string describing the chain inverts its order. Thus, processes I and II exchange their roles, as do III and IV. A systematic description of how the processes transform when mirrored with respect to a vertical (corresponds to the view of the colony "from below") or horizontal axis and rotated by 180° is given in [1.16].

1.3 Results

1.3.1 Separation processes

1.3.1.1 Observation of the separation processes

When the formation of daughter cells is completed, the opening of the neighboring

diatoms occurs before the next division can be seen. Thus, no more than two parallel connected diatoms occur, as is often observed in *D. vulgaris* or *Diatoma ehrenbergii*. Similar to *D. vulgaris* or *D. ehrenbergii*, in phase-sensitive light microscopic techniques, such as DIC, EPS pads after splitting are observed only at the connecting points of the diatoms (see Figure 1.1), but not at the unconnected apices. If one observes the development of colonies with respect to the division processes according to Figure 3, the difficulty therefore arises that one cannot clearly assign a type to the outer diatoms. In the case of a star-shaped colony of three diatoms, only the type of the middle diatom is known. With the orientation of the colony according to Figure 1.1 this is the type *d*. This diatom always divides into the sequence *ab* according to process VII. The process of products a and b can be followed, and one observes processes II and III, i.e.:

$$\begin{aligned} d &\rightarrow a\ b \qquad (VII) \\ a &\rightarrow d\ a \qquad (II) \\ b &\rightarrow b\ d \qquad (III) \end{aligned} \tag{1.1}$$

There was no deviation from these rules in subsequent generations or in any other colonies studied. A diatom of type *c* is never formed in these processes and, indeed, no colony is found in which both non-diagonal types occur simultaneously. These rules were derived solely from the observed division of type *d*. Assuming that the adjacent diatoms of a star-shaped colony divide according to the same rules, one recognizes that they always have a diagonal type, so that the initial colony can be described by the string *bda*.

Looking at a colony from a view rotated by 180°, in which type *c* occurs, the observed processes are:

$$\begin{aligned} c &\rightarrow b\ a \qquad (V) \\ a &\rightarrow a\ c \qquad (I) \\ b &\rightarrow c\ b \qquad (IV) \end{aligned} \tag{1.2}$$

One can obtain these results by rotating the processes (1.1), but also a vertical mirroring (horizontal mirror axis) leads to this outcome. There is a view in which processes occur according to the rules (1.1) with *d* as non-diagonal type a second view according to

(1.2) with *c* as non-diagonal type. As diatoms develop independently, apparently the diagonal types have a hidden asymmetry with respect to the horizontal, which is passed on to daughter cells. In three-dimensional space, this means an asymmetry with respect to the transapical plane. It is possible to extend the presented nomenclature to take into account the asymmetry in the types, as shown in the appendix. For the following considerations this is not necessarily required, because the views can be transformed in the mentioned way. In the following, a view of the colony according to processes (1.1) is assumed as a convention.

1.3.1.2 Lindenmayer system

The development of diatoms of a colony strictly follows the processes (1.1) or (1.2), respectively, but the appearance of a colony additionally depends on the times needed for the cell divisions, which are not necessarily identical. For the following considerations, we assume synchronicity of the divisions on the regarded section of the colony. Then the formation of the colony is given by a Lindenmayer system (L-system). An L-system is a triple ([1.22], [1.23]) consisting of:

- Alphabet
- Replacement rules (production rules)
- Initial sequence ω (Axiom)

The alphabet is made up of the set $\{a, b, c, d\}$. The replacement rules are described by the processes (1.1) or (1.2) depending on the perspective chosen. In the case of *D. tenuis* colonies, a simplification results if one fixes a view. If one considers the chain such that *d* is the non-diagonal element, one can restrict oneself to the reduced alphabet $\{a, b, d\}$ and the rules (1.1). Formally, one can use any string consisting of the letters of the alphabet as the initial sequence, but biologically only the sequences occurring in nature are meaningful, i.e., in particular, the letters of the alphabet representing individual diatoms (e.g., the initial cell).

The substitution rules are applied to the initial sequence (generation $G_0 = \omega$), creating a first generation G_1. By iteratively applying these rules, subsequent generations G_2, G_3, G_4, ... are formed. For simplicity, the term "generation" is also used here for the string that describes a generation.

Thus, there is a one-dimensional, deterministic, and context-free L-system (D0L-system) [1.27]. Context-free means that the replacement rules depend only on one element, but not on their neighbors. Because of this property, one can also compute the formation of a section of a colony without looking at its neighborhood. This is important because the observed colonies in *D. tenuis* represent fragments of previous colonies.

Already in 1987, a one-dimensional L-system was successfully applied by Koster and Lindenmeyer for describing the size sequence in the cyanobacterium *Anabaena catenula* [1.10]. One-dimensional L-systems are used in the context of diatoms to calculate the size sequence of diatoms in clonal colonies ([1.43] and [1.17]), as well as pattern formation in *D. vulgaris* [1.16]. More complex L-systems allow the generation of a wide variety of plant structures (see Prusinkiewicz [1.36]).

1.3.1.3 Sequence of diatom types

If one begins the formation of the cultures according to the rules of the L-system with a single diatom, then it is without importance whether one begins with the type *a* or *b*. The types *a* and *b*, as well as the processes II and III change into each other by mirroring at the vertical and because of the mirror symmetry of the process VII also the sequences of the generations of *a* and *b* are mirror images of each other. The type *d* provides the concatenation of the sequences generated from *a* and *b* because of $d \rightarrow ab$. With the initial value *a* and the processes (1.1), we obtain:

$$
\begin{aligned}
&G_0 = a \\
&G_1 = d\ a \\
&G_2 = a\ (b\ d\ a) \\
&G_3 = d\ a\ (b\ d\ a)(b\ d\ a) \\
&G_4 = a\ (b\ d\ a)\ (b\ d\ a)(b\ d\ a)\ (b\ d\ a)(b\ d\ a) \\
&G_5 = da\ (b\ d\ a)(b\ d\ a)(b\ d\ a)(b\ d\ a)(b\ d\ a)(b\ d\ a)(b\ d\ a)(b\ d\ a)(b\ d\ a)(b\ d\ a) \\
&\ldots
\end{aligned}
\tag{1.3}
$$

From generation G_2 onwards, we recognize the appearance of the star-shaped structure, which shall be denoted by S ($S = bda$). For structuring purposes, they have been grouped together in brackets, which have no semantic meaning. For simplicity, a chain consisting of k connected star-shaped colonies will be denoted kS. Except for the

beginning of the sequence, which alternates between *a* and *da*, a sequence of connected stellate structures emerges. As the number of diatoms doubles with each iteration, the two elements at the beginning of each generation hardly play a role in the overall picture of a real culture. Star-like structures generate two connected stars $1S \rightarrow 2S$ within one iteration according to the replacement rules. This development is illustrated in Figure 1.4. To illustrate the formation, the divisions of the middle diatom and those of the outer diatom were not shown simultaneously, but sequentially, even though this does not correspond to the assumption of a synchronous division.

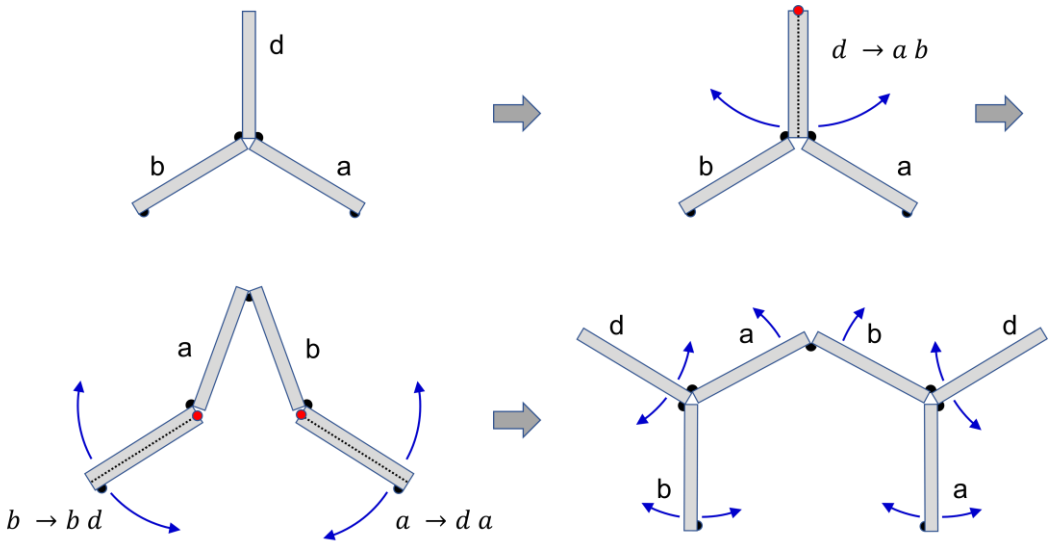

Figure 1.4 Shown is the evolution of the star-shaped colony within one iteration according to $(\boldsymbol{bda}) \rightarrow (\boldsymbol{bda})(\boldsymbol{bda})$. The order of divisions was chosen arbitrarily. Depending on the order, different transitional forms arise. In the colony $(\boldsymbol{bda})(\boldsymbol{bda})$ the separations were marked, which in the next generation lead to four connected stars.

The small red circles indicate where the connecting EPS pad is located in the upcoming separation. To assign types to diatoms, note that diagonal types a and b can be rotated to an orientation as in Figure 1.2. If one performs an additional iteration, four connected star-shaped colonies are formed in the subsequent generation.

1.3.2 Breaking of colonies

1.3.2.1 Frequency of the colony forms

The vulnerability to breakage in diatom colonies varies among species, and breakage as a result of grazing and flow can have an effect on chain length ([1.45] [1.29]). Some marine diatom species are capable of reducing their chain lengths when stressed by grazing [1.37]. A simple experiment demonstrates that rapid ejection of a sample

through a narrow-opening pipette in older *D. tenuis* cultures is sufficient to produce a large number of fragments of widely varying sizes. However, in *D. tenuis*, spontaneous chain breaks also occur in cultures where there is only a very low flow velocity, caused by thermal convection. In observations in cultures as well as water samples, no chains of more than 12 diatoms are found, so that chain breakage must always occur before the formation of larger structures. Specifically, one observes star-shaped colonies consisting of three diatoms and connected star-shaped colonies with up to four such stellate structures, as well as colonies in transitional forms. As observations show, colonies in transitional states also break and contribute to smaller irregular fragments. Thus, in addition to the rules for generating the sequence of types, breakage of *D. tenuis* colonies is an essential intrinsic mechanism for structure formation.

Cultures with exponential growth have a characteristic frequency distribution of shapes. Figure 1.5a shows a histogram obtained by counting 1539 colonies in an exponentially growing culture (generation time about 980 minutes) of low density. All colonies with the same number of diatoms were grouped together so that different structures could contribute to one column. Among colonies with three diatoms, one out of a total of 123 colonies was not star-shaped (*abd* or *dab*), and among colonies with six diatoms, five out of 1140 were not type 2*S*. The highest proportion of "non-regular" structures is found in colonies formed by nine diatoms. Only four of 18 colonies consisted of connected stellar structures. In addition, four of the five colonies with 12 diatoms were formed from four stars. The proportion of 4*S* structures is higher than in the case of 3*S*, but the absolute number is so small that it is not noticeable in the histogram. In all observations on exponentially growing cultures, the 2*S* structures clearly dominated. The second most common form was simple star-shaped colonies (1*S*).

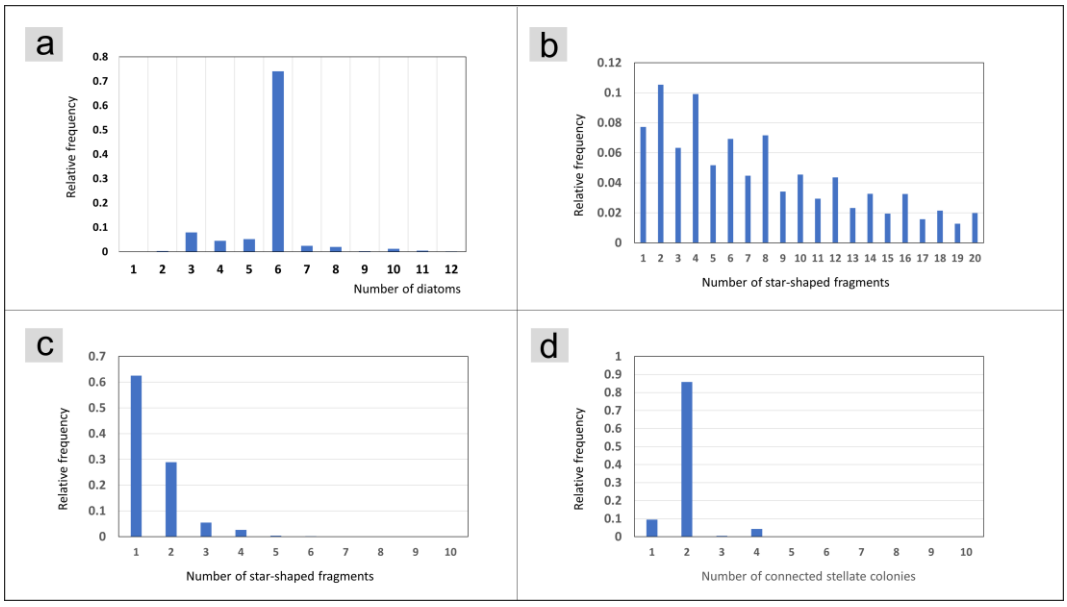

Figure 1.5 (a) Normalized frequency of the number of diatoms in a colony observed in a culture in exponential growth. (b) Theoretical frequency of *k*S colonies, where *k* indicates the number of star-shaped fragments in a colony. A low constant fragmentation probability was assumed. (c) Simulation as in (b), but with high fragmentation probability. (d) Simulation with some suitably chosen probabilities.

The distribution is different for cultures that entered the stationary phase due to lack of resources, i.e., where the generation time increases strongly. Here, the proportion of single star-shaped colonies increased continuously with the age of the culture and clearly exceeded that of double star-shaped colonies.

1.3.2.2 Importance of the size limit of a colony

A simple observation of sinking *D. tenuis* colonies in a Petri dish shows that single and double star-shaped colonies sink predominantly in a horizontal orientation in turbulence-free water, exhibiting comparable sinking speeds. At the typical angles between neighboring diatoms of about 120°, the structure of the colony becomes closed at three stars. In the case of four connected stars, as it occurs in the subsequent generation of the double star structure, the diatoms of a colony can already collide when arranged in the plane and form irregular structures due to spatial limitation. As the frequency distribution in Figure 1.5a shows, these structures occur only rarely, which is interpreted as an indication of disadvantages in a planktonic lifestyle. Even larger colonies are completely avoided.

1.3.2.3 Observed breaking points

Without application of external forces, colonies break up only between type *a* and *b*

diatoms, i.e., at locations in the colony with the sequence *ab*. These are the connection points of star-shaped colonies (see generations according to (1.3)). In contrast, the connection points with sequences *bd* or *da* are stable. Therefore, a 2*S* colony always separates into two 1*S* colonies in case of a break, which preserves the ideal star-shaped structure. In a 4*S* colony, there are three possibilities for a break, with the most common break occurring in the middle of the colony, giving rise to two 2*S* structures. In a view according to Figure 1.2a, all possible separation points are in the upper band. As no type *c* elements are possible in the chosen view, only *ab*-contacts are found in this band. Thus, there is an apical side to the diatoms whose connections are always also potential breaking points.

1.3.2.4 Consideration of the breaking points in the L-system

It is postulated that the dynamics of the breakage of an *ab*-connection depends on the length of time between the formation of an *ab*-connection and its breakage, and that no exchange of information between diatoms about the size of the colony is required. For the investigation of the probabilities of the temporal behavior of the breakages, the age of the *ab*-connection points is to be introduced in units of generation times. Consistent with modeling by an L-system, we restrict ourselves to the times at which the generations are formed, so no continuous variable is needed. An *ab*-connection arises according to (1) by the process $d \rightarrow ab$. The rules according to (1.1) do not allow any other generation of this sequence. It is also essential that, according to the production rules (1.1), an *ab*-transition is preserved in successive generations ($ab \rightarrow d\boldsymbol{ab}d$). We supplement the alphabet to $\{a, b, d, \mathbb{N}_0\}$, where $\mathbb{N}_0$ denotes the set of natural numbers including zero. For considering the age of the *ab*-connections, the production rules are extended as follows:

$$\begin{aligned} &d \rightarrow a\ 0\ b \quad (VII)\\ &a \rightarrow d\ a \quad (II)\\ &b \rightarrow b\ d \quad (III)\\ &k \rightarrow k+1\ mit\ k \in \mathbb{N}_0 \end{aligned} \tag{1.4}$$

Each time an *ab*-connection is created, 0 is entered as the age of the connection. According to the last rule, the age is incremented in each subsequent generation. The analogous representation for the view according to (1.2) is omitted. Using (1.4), we

obtain the substitution rule $S \rightarrow S0S$. If we start with axiom a, we get for example for the fifth generation:

$$d\,a\,1\,S\,0\,S\,3\,\boldsymbol{S\,0\,S\,1\,S\,0\,S\,2\,S\,0\,S\,1\,S\,0\,S} \qquad (1.5)$$

If one begins the development with an *S*, then a symmetrical string arises, as it is contained in the above development (bold printed). It emerges from the *S* of the second generation $G_2 = a\,S$.

1.3.2.5 Frequency of colony forms and Monte Carlo simulation.

If axiom *a* or *b* is taken as a basis, the first possible breaking point arises with the formation of the 2*S* structure in the third generation. In synchronous divisions, another generation time passes until 4*S*. We consider a larger ensemble of colonies in synchronous division. Let the probability that an *ab*-connection breaks already within the first generation time after its formation be denoted by p_1, so that at the time of formation of the next generation the complementary part is maintained with probability $1 - p_1$. Correspondingly, let p_k be the probability of a break between the (*k*-1)th and *k*th generations after the formation of an *ab*-connection. Assuming statistical independence, the probability of a connection existing after *k* generations since formation is given by $Q_k = (1 - p_1)(1 - p_2) \ldots (1 - p_k)$ and the complementary probability of a break by $1 - Q_k$.

Under model assumptions of certain values for p_k, the expected chain lengths can be estimated numerically with the help of a Monte Carlo simulation. For this purpose, a long chain (18 iterations were used) is calculated with the rules of the L-system (1.4). At the possible breaking points, according to the age of their formation, given by the index *k*, it is determined by means of a random process whether a break occurs. The lengths of the fragments are then determined, and a histogram is formed over the length of the colonies. To achieve low statistical fluctuations, an average is taken over a larger number of simulations runs (typically 100).

A simple assumption would be that the probabilities for a decay in a generation time are constant, that is $p = p_k$, as known from radioactive decay. This assumption is made in [1.14] and describes well the colony length in *Phaeodactylum tricornutum*. There is no aging of the connection points, and the existing proportions of the connection points drop exponentially because $Q_k = (1 - p)^k$. At the same time the

connection points double in each generation. One can achieve that there are more 2*S* than 1*S* structures by choosing *p* small. A simulation with $p = 0.05$ is shown in Figure 1.5b. In this case, very long chains and a characteristic structural pattern occur. If, on the other hand, a *p* close to 1 is chosen, long chains do not occur, but 1*S* colonies are then predominant, because connections break mainly within the first generation, as shown in Figure 1.5c.

A more realistic picture in the context of the assumption of synchronicity requires a small p_1, so that only a few breaks occur until the formation of a 4*S* structure. Furthermore, $p_3 = 1$ so that larger colonies are no longer observable. For Figure 1.5d, $p_1 = 0.005$, $p_2 = 0.9$ and $p_3 = 1$ were chosen. As expected, almost only 2S colonies occur. When these have evolved into 4*S* colonies, they are very likely to break in half shortly after their formation, so that only a few 4*S* structures can be found. Indeed, one can observe these separations. With the parameters presented and the resulting small colonies, a large chain length is not required for simulation because of the self-similarity of the sequence. However, it is used to obtain a large number of events.

The described temporal behavior shows that it is neither an unchanged probability of breakage over time nor a slow reduction of the cohesive force, but rather a very rapid breakdown of the bond after a certain time. In observations of the separation processes, it is striking that they are often associated with a jerky change in the position of the two remaining fragments. The cause could be the presence of a mechanical stress of the in the area of the connection point immediately before disconnection.

When colonies no longer reproduce exponentially due to a lack of resources, i.e., the generation time increases continuously, then the probability that 2*S* structures separate before the formation of the next generation also increases. In a stationary culture, there are only separation processes, but no vegetative reproduction. However, a certain proportion of 2*S* structures seems to persist for a long time.

1.3.3 Synchronicity

1.3.3.1 Basic assumptions

Except for a few diatoms at the chain ends, the L-system is limited to the formation and separation of connected star-like structures, as synchronous divisions were taken as a

basis. Although each separation meets the division processes or production rules, a colony or a fragment of it cannot be described by a single generation if the time between cell divisions is not equal. Unequal doubling times lead to transitional forms that occur, at least temporarily, between stellate structures (see Figure 1.5a). It is to be examined to which degree synchronism is given.

A synchronization of the divisions can happen by periodic influence of environmental parameters. The alternation of brightness and darkness by the day-night rhythm can induce this. However, a favorable choice of periodic light exposure is more successful ([1.34], [1.30], [1.31]). Furthermore, synchronicity can be achieved by periodic silicate addition in cultures maintained under silicate deprivation ([1.21], [1.5], [1.8], [1.9]). In the *D. tenuis* cultures, no synchronization with periodic illumination (a light-dark cycle in 24 hours) could be observed. Global synchronism within a culture is not required for the emergence of the observed *k*S structures. It is sufficient if there is adequate synchronism of divisions from a single diatom to the formation of a chain of four star-shaped colonies.

Doubling time is to be understood as the period between successive vegetative cell divisions. The generation time is the mean doubling time within the culture. It depends on environmental parameters such as nutrient concentration, light intensity or temperature, which are assumed to be homogeneous within the culture. The doubling time is a stochastic quantity that can be characterized by a density function [1.11]. Let its expected value, i.e., the generation time, be μ and its standard deviation σ. In the following, we will assume that successive doubling times are statistically independent, which is not true for all species [1.18]. In addition, we assume that the statistical properties of daughter cell doubling times are identical. This assumption is also not always fulfilled [1.20]. If we approximate the density function of the doubling time by a normal distribution, it is given by:

$$\mathrm{f}_1(t) = \frac{1}{\sqrt{2\pi\sigma^2}} e^{-\frac{(t-\mu)^2}{2\sigma^2}} . \tag{1.6}$$

Considering k consecutive divisions starting from one diatom, where the doubling times are $t_1, t_2, .. t_k$, the density distribution of the total period $t = \sum_{i=1}^{k} t_i$ is given by convolutions of the density function [1.13]. Again, a normal distribution is obtained:

$$\mathrm{f}_k(t) = \frac{1}{\sqrt{2\pi k\sigma^2}} e^{-\frac{(t-k\mu)^2}{2k\sigma^2}} \tag{1.7}$$

where the mean is given by $\mu_k = k * \mu$ and the standard deviation by $\sigma_k = \sqrt{k}\sigma$. Even if $\mathrm{f}_1(t)$ deviates from a normal distribution, the density distribution $\mathrm{f}_k(t)$ approaches the normal distribution with increasing *k* due to the central limit theorem. The mean values of the density functions are equidistant, while the standard deviation increases with increasing number of divisions, so that the curves $\mathrm{f}_j(t)$ and $\mathrm{f}_{j+1}(t)$ overlap more and more as *j* grows. With strong overlap it is no longer unlikely that a *j*+1th division precedes a *j*th division.

1.3.3.2 Observation of synchronism

In a long-term observation, doubling times were recorded. The observation covered a light phase and a dark phase, with the LED illumination of the inverted microscope switched on in addition to the culture illumination. It was found that in the dark phase (microscope illumination only), doubling times increased by approximately 5%. Therefore, only the observed divisions of the light phase were used for the following results. The mean of the 23 doubling times was 983 minutes, and the standard deviation was 47.32 minutes, so that $\sigma/\mu = 0.048$. These values are used as a basis in Figure 1.2, which shows the functions $f_1(t)$ to $f_5(t)$. In each curve, the range $\mu_k \pm \sigma_k$ is marked by a horizontal line segment, within which 68.27% of all *k*-th divisions lie. The dotted line segment below denotes the range $\mu_k \pm 2\sigma_k$. About 95.45% of all divisions lie within this range.

1.3.3.3 Synchronicity and probability of breakage

We consider the subsequent generations of a diatom of type *a* (generation G_0), as it was assumed in the calculation (1.3). This cell has an age given by the duration since the last cell division (separation at time $t = 0$). In the interval in which it is not yet divided with very high probability, it is visualized in Figure 1.2 as a short line (one diatom of type *a*). Correspondingly, there is a region between the maxima of f_1 and f_2 in which the colony $G_1 = da$ is observed with a very high probability. This continues accordingly, with the intervals between successive maxima in which (almost) no separations occur becoming smaller and smaller as the distribution functions increases. The colony forms are drawn

in the intervals. Transitional forms are located in the areas between the intervals. The existence of such non-overlapping intervals up to a certain maximum generation justifies the assumption of sufficient synchronicity over this period. On the other hand, the broadening sections containing separations indicate the limitation of the description by an L-system.

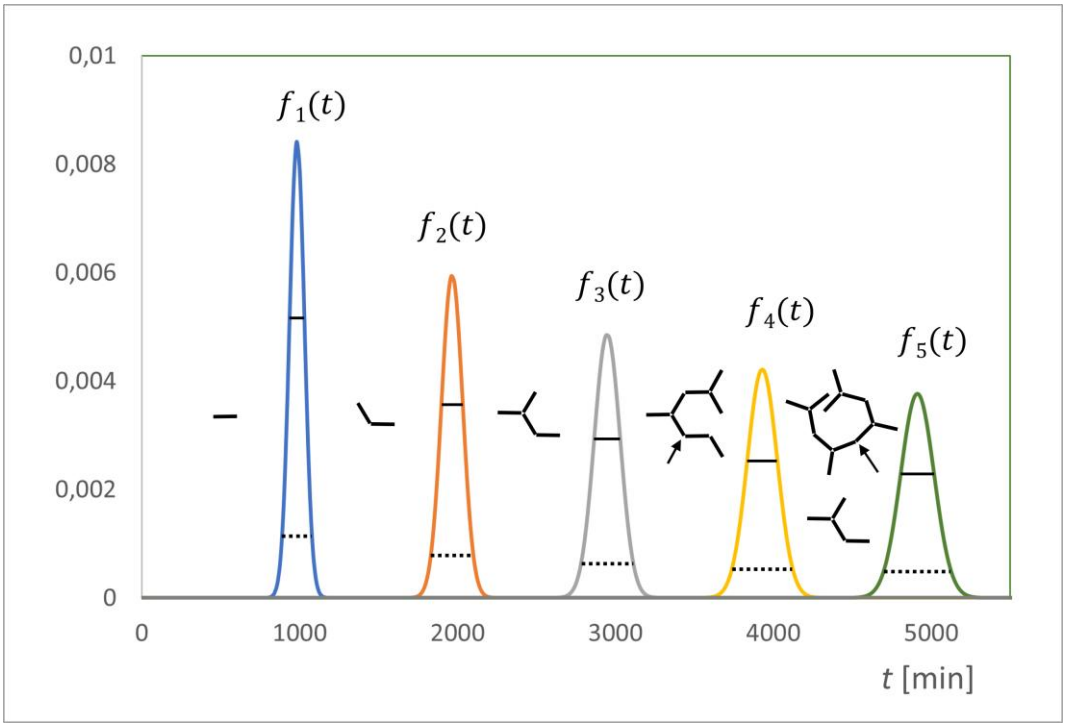

Figure 1.6 Density functions for the first to fifth divisions starting with a single diatom. The forms of the colonies are illustrated in the sections where there is a high probability that no divisions occur. In the intervals between the maxima of $f_k(t)$ and $f_{k+1}(t)$ one finds the forms of the generation G_k, in the region of the maxima the transition forms between them.

The first *ab*-connection appears in the generation $G_2 = a(bda)$. It is marked with a small arrow in the subsequent generation $G_3 = da(bda)(bda)$. According to the rules for colony breakage, the separation into *da* and the 2*S* structure occurs with high probability before the beginning of the formation of generation G_4. Therefore, the break in G_4 has been drawn so that a 4*S* colony is formed. Similarly, another arrow is drawn in G4, leading to the formation of two 2*S* structures before G_5. A possible breaking of *ab*-connections into two 1*S* structures after one generation was not considered in Figure 1.6.

As the breaks already occur after a few generations, one can also start the considerations with a diatom which is part of a colony. It always creates a 4S structure that quickly breaks. Each diatom in a colony is the starting point of a development as shown in figure F6. Although the synchronous sections between successive density

functions become increasingly narrow, leading to a loss of global synchronization in a culture, this is irrelevant for the observed structures because of the breakup of the colonies.

1.3.4 Angles between neighboring diatoms

1.3.4.1 Influence of the angles on the sinking speed

The sinking speed of phytoplankton is well described by Stoke's law because of small Reynolds numbers. Besides the density difference of phytoplankton and surrounding water, it depends essentially on the shape of the sinking body. The ratio of sinking speed $v_s$of a considered body to that of a sphere with the same volume and density v_0 is given by $v_s = v_0/\Phi$ with the dimensionless form resistance Φ, which depends on the shape of the body. Modifications of Stoke's law presented in [1.26] will not be taken into account here.

In the experimental study of Judit Padisák et al. [1.32] the sinking speed of differently shaped models, including star-shaped *Asterionella* colonies, was measured in glycerin. The form resistance for a symmetrical colony of three diatoms (all angles between diatoms are 120°) was determined to be about 3.24 (value was taken from Figure 3 of this publication), so the sinking speed is reduced by a factor of $1/\Phi = 0.307$ compared to the equivalent sphere. Because of the similar shape of the colonies, this can also be used for *D. tenuis*. Deviations from the ideal symmetry lead to a smaller form resistance, i.e. to increased sinking speeds. If we denote the angles by α_1, α_2 and α_3, as shown in Figure 1.7a, then the form resistance depends on two angles because of $\alpha_3 = 360° - \alpha_1 - \alpha_2$. In [1.32], a measure of the deviation from ideal symmetry is defined by:

$$A = \sum_{j}^{3} \left|\alpha_j - 120°\right| \tag{1.8}$$

This quantity takes the value 0° in the symmetrical case ($\alpha_1 = \alpha_2 = \alpha_3 = 120°$). The measured values of the form resistance as a function of A show large fluctuations, but have a clear tendency, which is characterized by a best fit line. Using the slope m taken from Figure 3 in [1.32], we obtain

$$\Phi = 3.24 + mA \tag{1.9}$$

where $m \approx$ -0.0033/degree.

As the sinking rates of 1*S* and 2*S* colonies differ only slightly at best, it is also favorable for 2*S* colonies to have only a small asymmetry in each of their stellate substructures. Two aspects of asymmetry will be considered:

- The distribution of angles reached after complete opening of adjacent daughter cells.
- The dynamic process of angle change after the separation of newly formed diatoms.

1.3.4.2 Distribution of angles and sinking speed

As angles asymptotically reach a final value, the study of the achieved symmetry was carried out on a culture that was already in a steady state. In such a state, no divisions occur and therefore no small angles are found. However, because of the slow approach to the final angle, it cannot be excluded that some angles may still change slightly. In total, the angles α_1 and α_2 of 500 simple stellate colonies were measured. Repeated measurements showed that the accuracy of the angle measurement is less than one degree. The distribution of angles α_1 and α_2 are to be assumed identical for symmetry reasons, especially because no specific view can be defined. Figure 1.7b shows a histogram of the frequencies of the measured angles. The mean value of the 1000 angles is 121.5 degrees and the standard deviation amounts to 8.44 degrees. A normal distribution with these values is plotted in the diagram. For each colony, the parameter *A* of the asymmetry can be determined according to equation (1.8) and using equation (1.9) the shape resistance Φ. Since the sinking speed is of particular interest, a histogram of the relative frequencies of Φ^{-1} is shown in Figure 1.7c. Except for the scaling of the abscissa, this approximates the density function of the sinking speed.

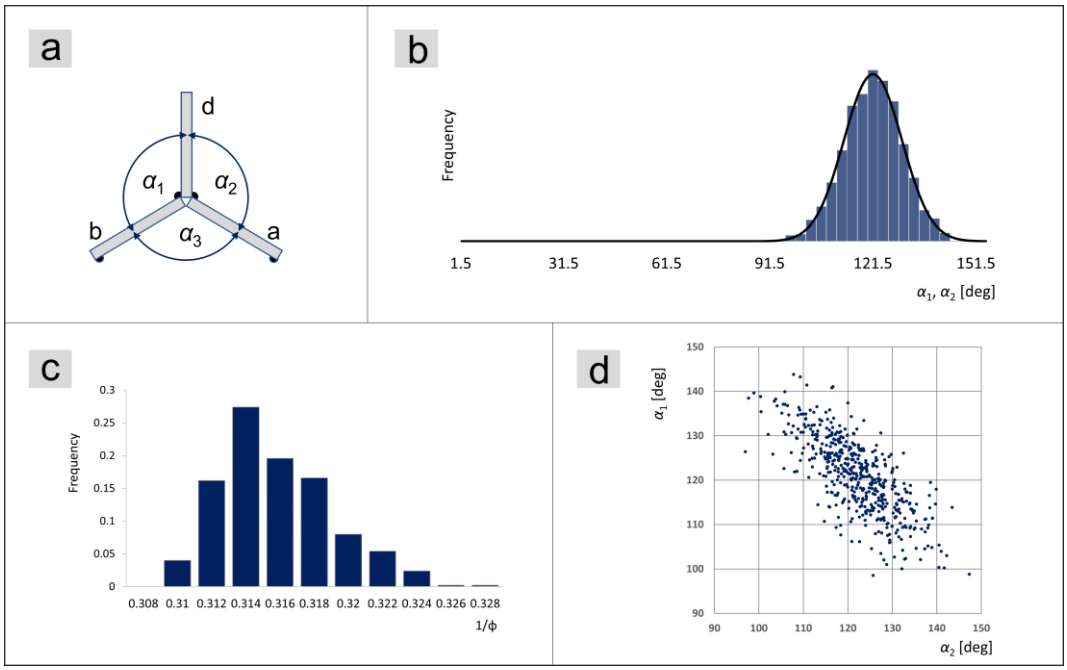

Figure 1.7 (a) α_1 and α_2 are the angles between diatoms connected by an EPS pad. (b) Frequency of the measured angles in a histogram where the bars have a width of 3 degrees. The normal distribution, parameterized by using the mean and standard deviation of the measurements, is a good fit to the histogram. (c) Histogram of $1/\Phi$ values obtained from 1000 measurements. (d) Scatter plot of α_1 and α_2. Each measured value is represented by a point in the plot.

The mean value of the values of $1/\Phi$ is 0.315 and the standard deviation is 0.00325. Thus, the mean value is just under 2% below the sinking speed in the case of ideal symmetry. Given the presumably high inaccuracies of the slope of the best fit line (1.9), this should be considered a rough approximation. However, it proves that the observed deviations from symmetry increase the sink rate only slightly.

If the diatoms of a star-shaped colony touch each other at the apical ends, they form a small triangle (see Figure 1.7a). If the diatoms have the same state in the division process (identical valve spacing of the diatoms), and the optimal angles are reached, i.e., $\alpha_1 = \alpha_2 = 120°$, this triangle is equilateral. This idealization is inaccurate even in the case of a culture in steady state, because one can see non-uniform developmental states and irregular EPS pads that do not connect the diatoms exactly at one point. In addition, the optimal angles are often not reached. As long as the diatoms do not touch each other, i.e., no such triangle is formed, the angles α_1 and α_2 can still increase. As soon as the diatoms touch at their apices, α_1 and α_2 can no longer grow unhindered and the angle $\alpha_3 = 360° - \alpha_1 - \alpha_2$ is mechanically limited, and thus, the sum angle $\alpha_1 + \alpha_2$. Plotting α_1 against α_2, as seen in Figure 1.7d, reveals an anticorrelation between α_1 and α_2 with a correlation coefficient of -0.743. Without such a constraint, one would expect the standard deviation of the remaining angle α_3 to be larger than that of α_1 or α_2, but it is

smaller (6.04°). The limitation of $\alpha_1 + \alpha_2$ probably contributes to an improvement of the symmetry properties.

1.3.4.3 Angle between neighboring diatoms as a function of time

The presented analysis of the angles was based on a culture in a stationary state, thus largely excluding the time-dependent splitting of newly formed daughter cells from consideration. The measure of asymmetry *A* can be used for quantitative evaluation of the dynamic development only in exceptions, as the splitting begins in the region of the transitions between the star-shaped structures, in which star-shaped structures of the next generation are just developing. In addition, it is likely that several such angular openings will occur overlapping in time, resulting in a very large number of possible forms. It is convenient to study the angle between neighboring diatoms as a function of time. If it reaches a value close to 120 degrees in a time interval that is small compared to the generation time, then the time interval in which the star-shaped structure exists (between the maxima in figure F6), will predominantly have a favorable configuration with a high form resistance.

As in *D. vulgaris* and *D. ehrenbergii*, the detachment of the diatoms starts with a sudden unfolding [1.16] into a V-shape. Since in video recordings at 30 fps this process always occurred completely between two frames, it should take considerably less time than 1/30 seconds. The extracellular polymeric substances extruded at the apical pore fields, which are not visible by light microscopy, must be liquid and, after formation of the adhesion, possibly build up a mechanical tension by interaction with the surrounding water, which then leads to spontaneous detachment of adjacent valvular surfaces (see discussion in [1.16]). After that, the angle starts to grow steadily. A typical example is shown in Figure 1.8, which shows the observed opening of a *bd*-connection (equivalent to *da*-connection).

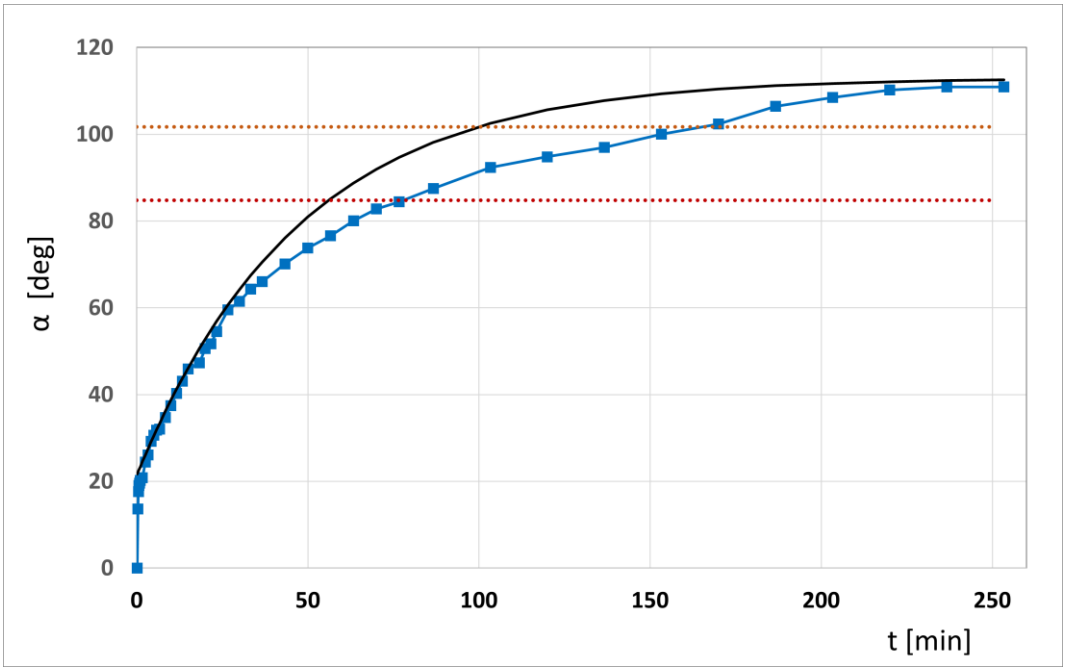

Figure 1.8 Typical function of the angle between diatoms as a function of time.

This development over time is part of the already described long-term observation, which also served to determine the doubling times and yielded a generation time of 983 minutes. One recognizes a step to about 14° at the beginning, which is quite typical. However, there is a larger variability here. An exponential function is plotted, based on the assumption that the change in angle is proportional to the difference from the final angle reached (in this case 113°) to the current angle. The proportionality factor was adjusted. In several observations, this proved to be a good approximation for the range of steep rise and flat rise for large times. Without exception, there was an irregular gradient below the exponential function in between, varying from observation to observation. The two dotted lines mark the reaching of 75% and 90% of the value at the end of the observation. In this measurement, they are reached after 77 minutes and 170 minutes. These are about 8% and 17% of the generation time. The irregular gradients lead to a strong variation of these reference values. Nevertheless, they were small compared to the generation duration in all observed cases.

1.3.5 Example of the formation of a colony

One example of a temporal development of a colony will be shown to illustrate the described aspects. Figure 1.9a shows a colony consisting of 10 diatoms, which represents a transitional form between a 2*S*-colony and a 4*S*-colony. It can be observed

when, starting from a 2*S* structure, all diatoms have divided except for the connecting *ab* elements (see Figure 1.4). Chronologically, this structure is in the region around the maximum of the density function $f_4(t)$ (see Figure 1.6). Therefore, a short time later, the two diatoms of types *a* and subsequently *b* separate, which can be seen in Figure 1.9b and Figure 1.9c. There are 22.66 minutes between these separations, which is 2.3% of the generation time. Note that the *ab*-pair was formed by $d \rightarrow ab$ at the same time and this occurred just one generation ago. In this case, both separations showed a large initial angle. Although the time difference between separations is small, the angle of separation $a \rightarrow da$ (on the left side in Figure 1.9c) is significantly larger than any of separation $b \rightarrow bd$ (on the right side in Figure 1.9c), indicating rapid opening compared to generation time. The result is a 4*S* colony which continuously varies in its outer shape by changing the angles (Figure 1.9c and Figure 1.9d).

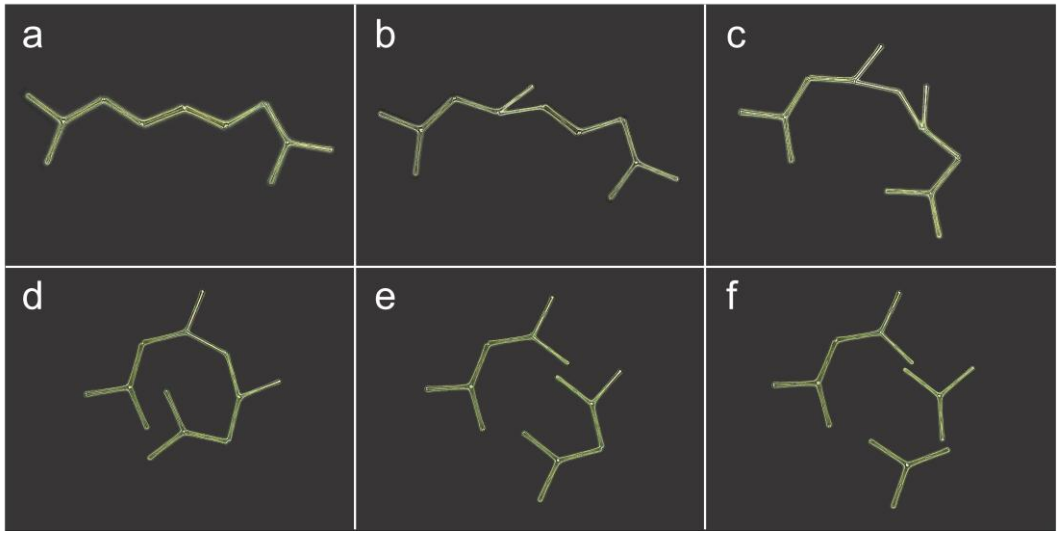

Figure 1.9 Time section of a development starting with a transitional form containing 10 diatoms. It comes from the long-term observation presented in section 1.3.3.2, where the generation time was 983 minutes.

The break in two 2*S*-structures (Figure 1.9e) occurs 102.7 minutes (10.4% of the generation time) after the formation of this structure, well before the next expected separation. Apparently, all angles of neighboring diatoms are already close to the ideal 120° for both 2*S* colonies. In most cases, the 2*S* colonies go through the same development to the 4*S* structure, but Figure F9f shows the case where one of the 2*S* colonies breaks into two 1*S* structures (55 min after the breakup of the 4*S* structure in Figure 1.9e). This is notable because the culture is in exponential growth.

According to the observed breakages in Figure 1.9e and Figure 1.9d, the ends at the breakage points are not located directly next to each other. Apart from tiny

displacements due to convection, this is caused by the offset at the moment of detachment. In the sequence of images, which is the basis of figure 9, a brief rotation of the colony in vertical direction (tilting to the optical axis) is also noticeable. Both indicate an active separation.

1.4 Conclusion

For the observed regular colony structures to form, several mechanisms and temporal boundary conditions must be satisfied:

1. Production rules for generating the *kS* structures,
2. Mechanism for breaking the chain at certain positions,
3. Appropriate timing of breakups to prevent large colonies,
4. Sufficient synchronism,
5. Low asymmetry in star-shaped colonies,
6. Rapid angular opening after completed cell division.

These criteria are not independent of each other. Production rules and disconnection points are jointly involved in pattern formation at colony level. The temporal conditions 3, 4 and 6 are related to the generation time. The mechanisms lead to the formation of *kS* structures with a maximum of $k = 4$, which decay rapidly. In all phases of the development of a culture, 1*S* and 2*S* structures dominate the appearance due to the breakage mechanisms. With the observed high symmetry, these structures lead to a large form resistance and thus a low sink speed. This advantage is lost if even one of the conditions is not met. For example, if larger colonies appeared, irregular shapes would be formed due to the mechanical constraints, resulting in a larger sinking speed. With the sinking of a large colony, many diatoms are lost at the same time.

The treatment of the pattern formation of the colony structure by an L-system does not distinguish between star-shaped or zig-zag-shaped structures. The identified L-system describes the structures of the concatenation that result from deterministic or stochastic selection of the processes. Thereby, a context dependence of neighboring diatoms is conceivable. Also, a memory in the form of a dependence of the choice of the processes on past processes, is imaginable. However, this modeling would go beyond the L-system.

Analysis of the processes can reveal asymmetries that are not reflected in the morphology of diatoms. For example, any preference for process I over process II demonstrates asymmetry. A symmetric model could be a non-deterministic L-system where the alternative processes are statistically independent and equally likely. A term for symmetry related to the processes of colony formation, analogous to "isopolar" at the level of valve structure, might be helpful.

A small subset of the colony formation choices is formed by the D0L-systems. Even nondeterministic systems may be approximated by a D0L-system, as has been shown for *D. vulgaris* [1.16]. With a selected view on a chain there are $2^4 = 16$ possibilities to pick the processes for the four types from Figure 1.2b. The number is reduced by the fact that symmetries occur which do not represent new systems but only other views. It should also be considered that not all types according to Figure 1.2b need to be present. The simplest possible D0L-system occurs in *Asterionella formosa*. The star-shaped colonies are formed by only one type, which is non-diagonal. If denoted by d, there is only $d \rightarrow dd$ as the relevant process (process VIII according to Figure 1.3d). The system is equivalent to the representation with the element c and the process $c \rightarrow cc$.

Assuming that life form is an evolutionary adaptation, identical L-systems across genera and species indicate similar environmental requirements. The colony form of *A. formosa*, for example, is also typical for other species that exhibit a planktonic way of life, such as *Tabellaria fenestrata*. Systematic studies could not be performed yet, but we hypothesize that the colony formation in *D. vulgaris* with respect to the deterministic approximation and benthic *Tabellaria flocculosa* are based on the same D0L-system. L-systems represent a classification that allows cross-references to be made between environmental requirements for different species. This classification differentiates more specifically than a zig-zag or star-shaped-colony categorization. However, as the comparison of the planktonic *D. tenuis* and *A. formosa* shows, the selection pressure of minimizing the speed of sinking leads to a similar appearance, but the rules of formation are different (convergent evolution). This is expressed in the fact that in *A. formosa* there are no chained stellate colonies and no transitional forms in terms of non-star-shaped colonies.

Other colony forms of *D. tenuis* [1.19] represent other adaptations and are probably enabled by the interaction of different mechanisms. As no structural changes of the colonies occurred during cultivation for more than one year, and thus the

processes, breakage mechanisms, and temporal relations remained unchanged, the question arises about varieties in a genetic sense or, alternatively, the environmental conditions influencing structure formation. In flowing waters, a chain with attachments to the substrate could be advantageous. It should be mentioned that in clonally cultivated *D. ehrenbergii*, large sessile zig-zag-shaped colonies and planktonic star-shaped colonies of three diatoms, as well as connected star-shaped colonies were found in coexistence in sufficiently dense cultures. The smaller planktonic colonies are formed when small colonies multiply, as well as by breaking off from the long benthic chains.

Apart from the continuously changing nutrient concentrations in batch cultures, the observations made were made under largely uniform environmental conditions. Further investigations could provide information on the dependence of generation time, breakage probability, angle opening etc. on environmental conditions such as light intensity, nutrient concentrations, and temperature. It is to be expected that from a change of one parameter the generation time and the fracture probability are not affected to the same extent, so that, for example, the proportion of 1*S* and 2*S* structures is altered. The situation shown is to be understood as an exemplary observation.

The phenomenological modeling presented follows observations and does not provide an explanation for the underlying physiological mechanisms at smaller size scales. Clarification is needed in particular:

- The nature of asymmetry with respect to the transapical plane. *D. tenuis* is described as isopolar but has a rimoportula located near an apex. A relationship with this asymmetry would be a possible hypothesis.
- The formation of the EPS pads. The secretion of the EPS could occur on only one valve or both or could be initiated by one.
- The origin of the mechanical stress build-up that leads to the sudden opening of the daughter cells into a V-shape and the chemical or physical processes that play a role in this process.
- The mechanism of the breakages and the forces involved. The jerky separation suggests that it is an active separation in which one or both adjacent diatoms control the existence of the connection and separate the connection when it reaches a certain age.

According to the observations [1.14], very short chains do not occur in *Chaetoceros*

decipiens. In their model, the authors assume that separations do not take place when the distance to a chain boundary falls below a certain number of cells. To explain this, a cell-to-cell communication process is discussed, in which a diatom receives information about the chain. The mechanism for separation presented here is based only on the local information of age. It also allows the avoidance of short chains by assuming a minimum age of connections for breaking. It is possible that this is also an explanatory model for other colony-forming organisms. Controlled breaking of colonies also offers the possibility of adjusting the duration of a link's existence to the current generation time. This could explain why a certain proportion of 2*S* structures persist in *D*. *tenuis* of a stationary culture.

Appendix

Modeling the asymmetry

One method to model the asymmetry of chain formation is to extend the types and symbols presented. Analogous to the procedure in [1.16], an arrow is added to the element *a* pointing to the apex where the EPS pad is formed in the next division, as shown in Figure 1.10.

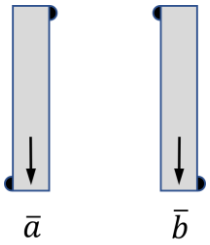

Figure 1.10 Diagonal types with information about orientation

The corresponding notation $\bar{a}$ refers to a position in the coordinate system as chosen in Figure 1.10 for the representation of the string. Only one diagonal element is needed, because an element corresponding to the representation of *b* is obtained by reflection on the vertical. In this position it is denoted as $\bar{b}$ (Figure 1.10). Oriented elements with arrow pointing upwards are obtained by rotating the elements by 180° with the same viewing direction. The element *d* is asymmetrical to the horizontal and mirror symmetrical to the vertical axis and can be converted to *c* by mirroring at the horizontal or rotation by 180°. A marking to indicate an orientation of this element is not necessary in *D*. *tenuis*. One non-diagonal and one diagonal type is sufficient for

description. With these definitions, the observed processes (1.1) can be represented in a uniform manner, taking orientation into account, as shown in Figure 1.11a to Figure 1.11c.

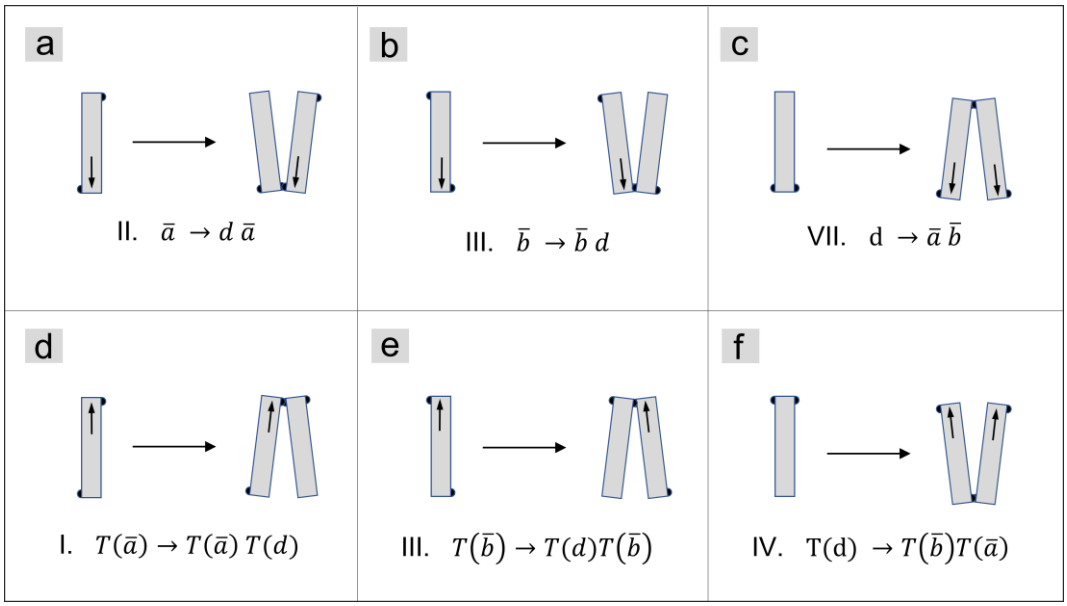

Figure 1.11 (a) The direction of the arrow in process II (Figure 11a) is maintained in the product generated, as the next division follows the same rule. (b) If process II is mirrored on the vertical, process III is generated. (c) The products at process VII must have the orientations shown so that the subsequent processes II and III are carried out correctly. (d), (e), (f) These processes are created by rotating 180° from the processes shown above.

If one rotates the view of the chain by 180° so that it is in inverse sequence in front of one, one obtains the processes according to (1.2) as shown in Figure 1.11d to Figure 1.11f. T stands for the operator of the rotation. For the rotated diagonal elements, one could introduce own identifiers. This is not necessary in the context of the description.

In practice, one recognizes the orientation of the chain by the occurrence of *c* or *d*. Only in the case of very short chains or single diatoms, one must follow the development until a non-diagonal element appears. Then one can take a preferred orientation. Therefore, this explicit representation of the asymmetry is mainly of formal interest. However, it shows that two types ($\bar{a}$ and $\bar{d}$) and two processes (II and VII) are sufficient, and all other types and processes can be generated by mirroring and rotation.

References

1.1: Agardh, C.A. (1812) Algarum decas prima. *Litteris Berlingianis, Lundae. 56 pp.*

1.2. Arrieta, J., Jeanneret, R., Roig, P., and Tuval, I. (2020). On the Fate of Sinking Diatoms: The Transport of Active Buoyancy-Regulating Cells in the Ocean.

Philosophical Transactions of the Royal Society A. *378*(2179), 20190529. doi: 10.1098/RSTA.2019.0529

1.3: Bahulikar, R.A., and Kroth, P.G. (2007) Localization of EPS components secreted by freshwater diatoms using differential staining with fluorophore-conjugated lectins and other fluorochromes. *European Journal of Phycology*, *42*(2), 199-208.

1.4. Birger Skjelbred, Nordic Microalgae (2014), http://nordicmicroalgae.org/taxon/Diatoma%20tenuis?media_id=Diatoma%20tenuis_6.jpg

1.5. Busby, W.F. and Lewin, J. (1967) Silicate uptake and silica shell formation by synchronously dividing cells of the diatom *Navicula pelticutosa* (Breb.) Hilse. *Journal of Phycology* 3, 127–131.

1.6. Celler, K., Hodl, I., Simone, A., Battin and T.J., Picioreanu, C. (2014) A mass-spring model unveils the morphogenesis of phototrophic *Diatoma* biofilms. *Scientific Reports* 4, 3649

1.7. Conway, K. and Trainor F. R. (1972) Scenedesmus morphology and flotation. *Journal of Phycology* 8: 138-143.

1.8. Darley, W. M. and Volcani, B. E. (1969) Role of silicon in diatom metabolism. A silicon requirement for desoxyribonucleic acid synthesis in the diatom *Cylindrotheca fusiformis* Reimann and Lewin. *Experimental Cell Research* 58, 334–343.

1.9. Davis, C.O., Harrison, P.J. and Dugdale, R.C. (1973) Continuous culture of marine diatoms under silicate limitation I. Synchronized life cycle of *Skeletonema costatum*. *Journal of Phycology* 9, 175–80.

1.10. De Koster, C. G. and Lindenmayer, A. (1987) Discrete and continuous models for heterocyst differentiation in growing filaments of blue-green bacteria. *Acta Biotheoretica* 36, 249–273.

1.11. Engelberg, J. and Hirsch, H.R. (1966) On the Theory of Synchronous Cultures. In: *Cell Synchrony*. I.L. Cameron and G.M. Podilla (eds.) Academic Press, New York, 14–37.

1.12. Falciatore, A., d'Alcalà, M. R., Croot, P., & Bowler, C. (2000). Perception of environmental signals by a marine diatom. *Science*, *288*(5475), 2363-2366.

1.13. Feller, W. (1971) *An introduction to probability theory and its applications.* Volume 2, 2nd edition, Wiley and Sons, New York.

1.14. Gherardi, M., Amato, A., Bouly, J. P., Cheminant, S., Ferrante, M. I., d'Alcalá, M. R., ... & Lagomarsino, M. C. (2016). Regulation of chain length in two diatoms as a growth-fragmentation process. *Physical Review E*, *94*(2), 022418.

1.15. Guillard, R.R.L. (1975) Culture of phytoplankton for feeding marine invertebrates. In: *Culture of Marine Invertebrate Animals*. W.L. Smith and M.H. Chanley (eds.) Plenum Press, New York, 26–60.

1.16. Harbich, T., Pattern Formation in *Diatoma vulgaris* Colonies in The Mathematical Biology of Diatoms [DMTH, Volume in the series: Diatoms: Biology & Applications, series editors: Richard Gordon & Joseph Seckbach]. J.L. Pappas and R. Gordon, (eds.) Wiley-Scrivener, Beverly, MA, USA: in preparation.

1.17. Harbich, T. (2021) On the Size Sequence of Diatoms in Clonal Chains In: Diatom Morphogenesis [DIMO, Volume in the series: Diatoms: Biology & Applications, series editors: Richard Gordon & Joseph Seckbach] V. Annenkov, J. Seckbach and R. Gordon, (eds.) Wiley-Scrivener, Beverly, MA, USA.

1.18. Hejblum, G., Costagliola, D., Valleron, A.J. and Mary, J.Y. (1988) Cell-Cycle Models and Mother Daughter Correlation. *Journal of Theoretical Biology* 131(2), 255-262.

1.19: Krammer, K. and Lange-Bertalot, H., Bacillariophyceae. 3. Teil: Centrales, Fragilariaceae, Eunotiaceae, in: *Süsswasserflora von Mitteleuropa*, vol. 2(3), H. Ettl, J. Gerloff, H. Heynig, D. Mollenhauer (Eds.), pp. 1–576, Gustav Fisher Verlag, Stuttgart, Germany, 1991.

1.20. Laney, S.R., Olson, R.J. and Sosik, H.M. (2012) Diatoms favor their younger daughters. *Limnology and Oceanography* 57(5), 1572–1578.

1.21. Lewin, J.C., Reimann, B.E., Busby, W.F. and Volcani, B.E. (1966) Silica shell formation in synchronously dividing diatoms. In: *Cell Synchrony*. I.L. Cameron and G.M. Podilla (eds.) Academic Press, New York, 169–188.

1.22. Lindenmayer, A. (1968) Mathematical models for cellular interactions in development: I. Filaments with one-sided inputs. *Journal of Theoretical Biology* 18, 290–299.

1.23. Lindenmayer, A. (1968) Mathematical models for cellular interactions in development: II. Simple and branching filaments with two-sided inputs. *Journal of Theoretical Biology* 18, 300–315.

1.24. Locker, F. (1950) Beiträge zur Kenntnis des Formwechsels von Diatomeen an Hand von Kulturversuchen. *Österreichische botanische Zeitschrift* 97, *322–2.*

1.25. Macdonald, J.D. (1869) On the structure of the diatomaceous frustule, and its genetic cycle. *Annals and Magazine of Natural History*. 4, 1–8.

1.26. Miklasz, K. A., and M. W. Denny (2010) MIKLASZ, Kevin A.; DENNY, Mark W. Diatom sinkings speeds: Improved predictions and insight from a modified Stokes' law. *Limnology and Oceanography* 55(6), 2513-2525

1.27. Mishra, J. and Mishra, S. (2007). *L-system Fractals*. Elsevier, 2007.

1.28. Naselli-Flores, L. & R. Barone, 2011. Fight on plankton! Or, phytoplankton shape and size as adaptive tools to get ahead in the struggle for life. *Cryptogamie, Algologie* 32: 157–204. https://doi.org/10.7872/crya.v32.iss2.2011.157

1.29. Nguyen, H. and Fauci, L. (2014) Hydrodynamics of diatom chains and semiflexible fibres. *Journal of The Royal Society Interface*, *11*(96), 20140314.

1.30. Paasche, E. (1967) Marine Plankton Algae Grown with Light-Dark Cycles. I. *Coccolithus huxleyi*. *Physiologia Plantarum* 20, 946–956.

1.31. Paasche, E. (1968) Marine plankton algae grown with light-dark cycles. 2. *Ditylum brightwellii* and *Nitzschia turgidula*. *Physiologia Plantarum* 21, 66–77.

1.32. Padisák, J., Soróczki-Pintér, É., and Rezner, Z. (2003) Sinking properties of some phytoplankton shapes and the relation of form resistance to morphological diversity of plankton—an experimental study. *Hydrobiologia* 500(1), 243-257.

1.33. Pfitzer, E. (1869) Über den Bau und die Zellteilung der Diatomeen. Bot. Zeitung 27, 774–776.

1.34. Pirson, A. and Lorenzen, H. (1966) Synchronized dividing algae. *Annual Rev. Plant Physiol.* 17, 439–58.

1.35. Potapova, M. Diatoms of North America (2010) https://diatoms.org/species/diatoma_tenuis

1.36. Prusinkiewicz, P. and Lindenmayer, A. (1990) *The Algorithmic Beauty of Plants*. Springer, New York.

1.37. Rigby, K. and Selander, E. (2021) Predatory cues drive colony size reduction in marine diatoms. *Ecology and Evolution*, *11*(16), 11020-11027.

1.38. Rimet, F. and Bouchez, A. (2012). Life-forms, cell-sizes and ecological guilds of diatoms in European rivers. *Knowledge and management of Aquatic Ecosystems*, (406), 01.

1.39. Round, F.E., Crawford, R.M. and Mann, D.G. (1990) *The diatoms: biology and morphology of the genera.* Cambridge University Press, Cambridge.

1.40. Smetacek, V. S. (1985). Role of sinking in diatom life-history cycles: ecological, evolutionary and geological significance. *Marine biology*, *84*(3), 239-251.

1.41. Sournia, A. (1982) Form and function in marine phytoplankton. *Biological reviews*, *57*(3), 347-394.

1.42. Spaulding et al. (2021) Diatoms of North America: Glossary, https://diatoms.org/glossary/setae

1.43. Ussing, A.P., Gordon, R., Ector, L., Buczko, K., Desnitskiy, A.G. and Vanlandingham, S.L. (2005) The colonial diatom ‘‘*Bacillaria paradoxa*’’: chaotic gliding motility, Lindenmeyer Model of colonial morphogenesis, and bibliography, with translation of O.F. Müller (1783) ‘About a peculiar being in the beach-water’. *Diatom Monographs* Vol. 5. Koeltz Scientific Books, Koenigstein.

1.44. Walsby, A. E., and Xypolyta, A. (1977) The form resistance of chitan fibres attached to the cells of Thalassiosira fluviatilis Hustedt. *British Phycological Journal*, *12*(3), 215-223.

1.45. Young, A. M., Karp-Boss, L., Jumars, P. A., & Landis, E. N. (2012). Quantifying diatom aspirations: Mechanical properties of chain-forming species. *Limnology and Oceanography*, *57*(6), 1789-1801.